

Surface structural and electronic properties of cleaved single crystals of $\text{Bi}_{2.15}\text{Sr}_{1.7}\text{CaCu}_2\text{O}_{8+\delta}$ compounds: A scanning tunneling microscopy study

C. K. Shih, R. M. Feenstra, J. R. Kirtley, and G. V. Chandrashekhar

IBM Research Division, Thomas J. Watson Research Center, P.O. Box 218, Yorktown Heights, New York 10598

(Received 14 April 1989)

Scanning tunneling microscopy is used to study the surface structural and electronic properties of cleaved single crystals of $\text{Bi}_{2.15}\text{Sr}_{1.7}\text{CaCu}_2\text{O}_{8+\delta}$. Images with atomic resolution reveal atomic chains with sinusoidal modulations running along the perovskite cell axis with a periodicity of nine to ten unit cells. These atomic chains stack along the **b** direction with a translational vector of one unit, resulting in an incommensurate periodicity of about 4.75 units along the **a** direction. In contrast to other reports, no evidence of "missing Bi-atom rows" is found. Spectroscopic studies show zero density of states at the Fermi level, implying that the surface Bi-O layer is nonmetallic.

The structural and electronic properties of high-temperature superconductors are currently under intensive investigation. Among the family of BiSrCaCuO compounds, the two layered materials with the nominal cation ratio of Bi:2 Sr:2 Ca:1 Cu:2 [referred to as the 2:2:1:2 compound, or Bi-Sr-Ca-Cu-O ($n=2$)] have attracted much attention. The primary reason for this relative popularity is the availability of large single crystals and the stability of the cleaved surface in vacuum.

In terms of the structural properties, most of the research on this compound concentrates on understanding the nature of the incommensurate superstructure, namely the existence of a long periodicity along one axis, which is often referred to as the **a** direction, equivalent to 4.75 times that of the fundamental tetragonal unit cell. Studies using transmission electron microscopy¹ have revealed certain qualitative features, such as the existence of in-plane and out-of-plane (relative to the *a-b* plane) lattice displacement. Furthermore, x-ray-diffraction analysis² has been used to deduce the modulation amplitude and periodicity. Previous analysis methods revealed only the bulk-averaged properties; it is therefore important to elucidate the real-space atomic nature of the incommensurate structure which is feasible with the scanning tunneling microscopy (STM). Up to now there has been only one STM analysis with atomic resolution shown by Kirk *et al.*³ In their work, a strong conclusion was drawn: A missing row of Bi atoms occurs either every nine or ten atomic sites, accounting for the incommensurate periodicity of the superstructure. However, as we report here, we do not find evidence for such missing atom rows.

In terms of electronic properties, photoemission spectroscopy (PES) and inverse photoemission spectroscopy (IPES) have been used to probe the filled and empty density of states. Although certain features have been assigned, much remains unknown. For instance, the states near the Fermi level observed in the PES (Ref. 4) and IPES (Ref. 5) have been identified as primarily oxygen *p* states. The question of whether these states originate from the Cu-O planes or other planes such as the Bi-O planes remains unanswered. Such questions are difficult to address using PES and IPES, since these techniques

average over about one unit cell perpendicular to the surface. On the other hand, the high surface sensitivity of the STM can be used to address these critical questions.

It is the purpose of this paper to simultaneously investigate the nature of the surface structural and electronic properties using STM. Structurally, we find that the surface atoms form atomic chains with sinusoidal modulations running along the perovskite cell axis with a periodicity of nine to ten unit cells. These atomic chains stack along the **b** direction with a translational vector of exactly one unit, resulting in an incommensurate periodicity of about 4.75 along the **a** direction. However, we do not find evidence for the missing Bi atom rows as proposed by Kirk *et al.*³ Electronically, our results show qualitative agreement with those reported using PES and IPES; however, we find very small density of states at the Fermi level, implying that the surface BiO layer is not metallic.

The experimental setup for our STM has been described previously.⁶ Single crystals of $\text{Bi}_{2.15}\text{Sr}_{1.7}\text{CaCu}_2\text{O}_{8+\delta}$ samples with T_c onset of 84 K were cleaved in an ultrahigh vacuum chamber with base pressure of $<4 \times 10^{-11}$ Torr. Based on symmetry considerations and other experimental evidence,⁷ single crystals of 2:2:1:2 compounds are most likely to cleave along the Bi-O plane. This assumption will be followed throughout our paper. All the studies were performed at room temperature. Low-energy electron diffraction (LEED) was performed either before or after STM studies to examine the surface orientation. STM images were acquired at a constant current of 100 pA. Spectroscopic data are taken by interrupting the feedback loop used for the topographic image, with the tip to sample separation (*s*) decreased as the sample bias is reduced in order to establish a large dynamic range (usually 4–6 orders of magnitude). The spectra are normalized as previously described.⁸

Figure 1(a) shows a top view of a typical STM image of cleaved Bi-Sr-Ca-Cu-O ($n=2$) surface taken at a sample bias of 1.75 V. We also indicate the corresponding perovskite cell axes which are referred to as [010] and [100], and the fundamental tetragonal cell axes **a** ([110]) and **b** ([110]). One can immediately observe atomic chains running along the [010] direction of the corre-

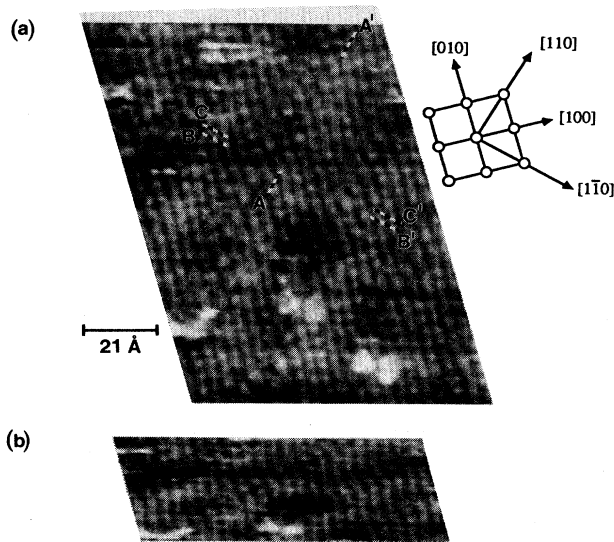


FIG. 1. (a) Top view STM image of a cleaved $\text{Bi}_{2.15}\text{Sr}_{1.7}\text{CaCu}_2\text{O}_{8+\delta}$ surface taken at a sample bias of 1.75 V. The perovskite axes are marked as $[100]$ and $[010]$, and the fundamental tetragonal axes a and b are labeled as $[1\bar{1}0]$ and $[110]$, respectively. The surface height is shown with a grey scale, ranging from 0 (black) to 2.5 \AA (white). Cross cut AA' is along b and cross cuts BB' and CC' are along the incommensurate direction a . (b) The same STM image compressed along the $[010]$ direction.

sponding perovskite cell. These chains have a lateral sinusoidal modulation which can be most clearly seen in Fig. 1(b) in which the image is compressed along $[010]$. The period of the modulation is about nine or ten unit cells and the modulation amplitude is measured as roughly $0.8 \pm 0.2 \text{ \AA}$ from side to side. Furthermore, these atomic chains stack along the b direction (i.e., the $[110]$ direction) with a translational periodicity of exactly one unit.

Since the modulation period along the $[010]$ direction has a component of $1/\sqrt{2}$ along $[1\bar{1}0]$, and the atomic distance along $[010]$ is $\sqrt{2}$ times that along $[1\bar{1}0]$, the modulation periodicity of nine or ten units along $[010]$ corresponds to a periodicity along a of 4.5 or 5 units. If one assumes that atoms are misplaced from their undistorted positions only along the a direction, then one has compressive and expansive atomic displacements along a and the displacement amplitude is 1.4 times the amplitude of the lateral displacement along the perovskite cell. On the other hand, there could be atomic displacement both along the a (compressive and expansive) and b (lateral) directions. In this case the displacement amplitude along a will be smaller than 1.4 times the lateral displacement amplitude along the perovskite axis. Based on the detailed analysis presented below, we find that the atomic rows along a mostly contain compressive and expansive displacements with very little lateral displacement.

In Fig. 2 we show the atomic corrugations along b and along the incommensurate direction a . Figure 2(a) corresponds to the corrugation along b marked as AA' in Fig.

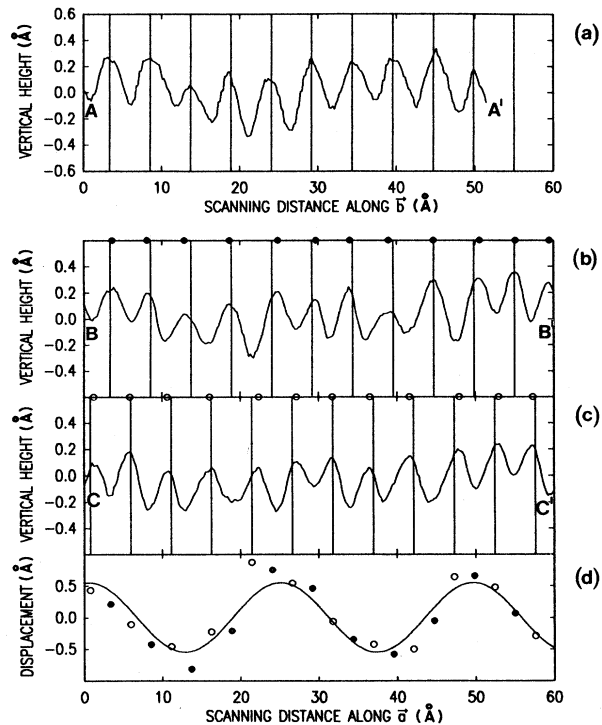


FIG. 2. Atomic corrugations along (a) AA' , (b) BB' , and (c) CC' cuts shown in Fig. 1. The equally spaced lines are marked in the figures. The maxima of the corrugations along BB' and CC' are also indicated on the top of each figure by using solid circles and open circles, respectively. (d) shows the atomic displacement along a for the atomic rows BB' and CC' . The first harmonic fit with the periodicity of 4.75 units is also shown.

1. Figures 2(b) and 2(c) show the corrugations of the two inequivalent neighboring atomic rows along a which are marked as BB' and CC' in Fig. 1. Equally spaced vertical lines are also drawn in these figures. As one can see from Fig. 2(a), the atomic spacing along the b direction is indeed a constant. Along BB' and CC' , one can find that the maxima deviate from the equally spaced lines with sometimes positive and sometimes negative deviations, resulting in compressive and expansive regions. Figure 2(d) shows the deviations from the equally spaced lines for BB' -type cuts (represented by solid circles) and the CC' -type cuts (open circles). The best-fit first harmonic with the periodicity of 4.75 units is also shown. The amplitude for the compressive and expansive modulation can be estimated from Fig. 2(d) as $1.1 \pm 0.3 \text{ \AA}$ from compression to expansion, which is very close to 1.4 times the lateral modulation amplitude ($0.8 \pm 0.2 \text{ \AA}$) along the perovskite axis. Thus we conclude that the atomic rows along a mostly contain the compressive and expansive displacements. The result of very small lateral displacement for atomic rows along a is consistent with the Bi-O in the bulk reported by Gao *et al.*² The displacement amplitude of 1.1 \AA in our work is very similar to that reported by Kirk *et al.*³ however, it is 40% larger than that reported by Gao *et al.*² using x-ray analysis for the Bi-O layer in the bulk. The vertical (out-of-plane) displacement in our im-

ages is only about 0.2–0.3 Å, which is similar to that of Gao *et al.*² and very different from that of Kirk *et al.*³ However, this value can vary greatly depending on the sample bias. Thus, one cannot infer the vertical displacement from images taken with a limited sample bias range.

Kirk *et al.*³ interpreted their STM images of 2:2:1:2 compounds in terms of missing atoms every nine or ten atomic sites. As one can see in Figs. 2(b) and 2(c), along both the BB' and CC' cuts, we do not find “missing” corrugation maxima. Similarly, the cuts along the perovskite axis do not show evidence of missing atoms. Kirk *et al.*³ have indicated that some of their images do not show the missing atoms, and attributed this to a multiple-tip effect. Of course, we cannot rule out the possibility of a multiple-tip effect existing in our measurement. However, even in the image from which Kirk *et al.*³ claim to see missing Bi-atom rows, one has at least a 50% probability of finding atoms in those “missing atom rows.” Moreover, in their atomic resolution image the sample was biased at 0.15 or 1.2 V, thus only states near the Fermi level contributed to the tunneling current. As suggested by the IPES work of Drube *et al.*,⁵ these states are primarily oxygen p states. Therefore, the image shown in their work is likely to represent the oxygen atoms. Based on the above discussions, the existence of the missing Bi-atom row should at least be considered as an open question.

We now turn to our spectroscopic studies. Figure 3 shows four typical spectra taken at different parts of the surface. There exist similarities and differences among these spectra. Generally, one finds much higher state density below -2 eV and above $+2$ eV than those in between, in other words, there is a gap region between -2 and $+2$ eV. Within this gap, various structures can be observed. The most consistent features are a peak at about 1.2 eV below the Fermi level, and a peak at between 1 and 1.5 eV above the Fermi level. Besides these two

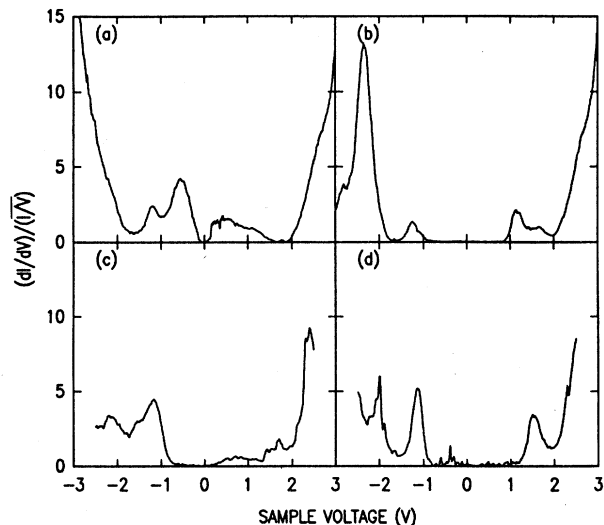


FIG. 3. Normalized conductivity vs voltage acquired at different parts of the cleaved $\text{Bi}_{2.15}\text{Sr}_{1.7}\text{CaCu}_2\text{O}_{8+\delta}$ surface. The sample voltage corresponds to the energy of an electronic state relative to the surface Fermi level.

features, in Fig. 3(a), one can also observe two peaks at about -0.6 and $+0.4$ eV. However, these two features are either completely missing [in Fig. 3(b)] or just barely observed. In all these spectra we always find zero conductivity at the Fermi level. Considering that the tunneling current in these measurements has spanned 5–6 orders of magnitude, it is very likely that the surface density of states indeed equals zero at the Fermi level.⁹

Variation of spectral features observed near the Fermi level in the spectra could possibly result from the varying electronic structure within the surface unit cell. Generally, our spectra were obtained with blunt tips, thus representing an average over a few atomic sites. The structural variation in the large supercell may still give rise to changes in the spectral properties, and sample inhomogeneities may also contribute to the observed variation. A more complete interpretation of the spectra requires detailed spatially resolved results.

It is very tempting to compare our spectroscopic results with the spectra obtained using PES and IPES, which are shown in Fig. 4. The IPES data shown here is after Drube *et al.*,⁵ and the PES data shown here is after Takahashi *et al.*⁴ We also choose our spectrum in Fig. 3(a) which shows most of the features to be compared with the PES and/or IPES results. For the unoccupied states, we find that there exist some consistent features between the

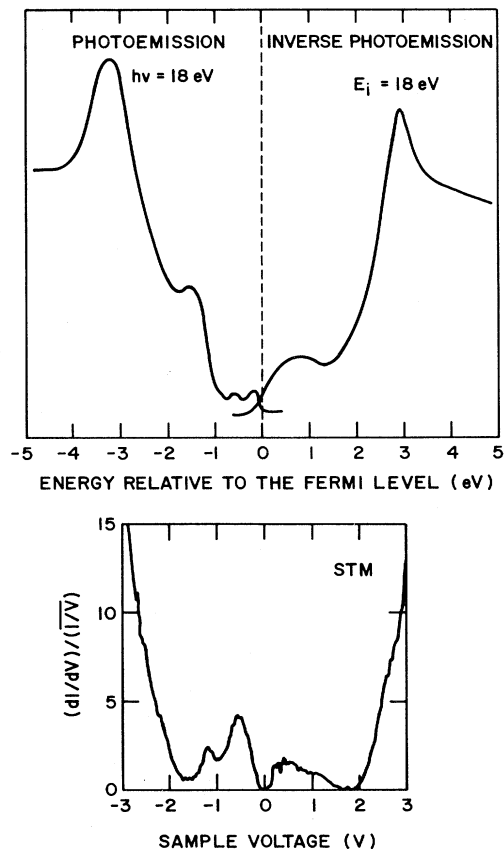


FIG. 4. Comparison of the STM spectrum and the spectra obtained by using PES (Ref. 4) and IPES (Ref. 5).

STM and IPES results. They both have a local minimum in the density of states (DOS) at about +2 eV, and very fast rising DOS above +2 eV. The DOS between 2 eV and the Fermi level also show qualitative agreement, except at the Fermi level. The states between 2 eV and the Fermi level have been identified by Drube *et al.* as the oxygen *p* states by investigating the resonant behavior of this feature. For the peak at 3 eV, based on the consistency with our STM result, it is suggested here as a Bi-related feature.

We now discuss the occupied states. Like the STM result, the PES spectra show a density of states which is low between the Fermi level and about -1.5 eV, and which then increases rapidly below -1.5 eV; however, the energy positions of features in the STM and PES spectra do not agree well. Furthermore, the PES spectrum shown in Fig. 4 is taken with a photon energy of 18 eV which enhances the emission of oxygen *2p* states. If we use the PES spectrum taken using photon energy of 74 eV, the agreement between the STM and PES is worse. We want to remind readers here that the IPES and PES probe a depth of about 20 Å, thus representing more of the DOS averaged over the whole unit cell, while the STM result represents only the DOS of the surface Bi-O layer. Due

to the complexity of the layered structures, in principle, one does not expect agreement between the STM and IPES and/or PES. The most important difference observed is the lack of density of states at the Fermi level in STM studies, implying a nonmetallic behavior of the surface Bi-O layer. Exact identification of other features discussed above will require further investigation.

In conclusion, we have used STM to study the surface structural and electronic properties of cleaved single crystals of $\text{Bi}_{2.15}\text{Sr}_{1.7}\text{CaCu}_2\text{O}_{8+\delta}$ compounds. Atomic images reveal atomic chains with sinusoidal modulation running along the perovskite cell axis. Detailed analysis shows that the atomic displacements along the incommensurate direction are primarily compressive and expansive. In our study we do not find evidence of the missing Bi-atom rows as reported by Kirk *et al.*³ Spectroscopy studies show that the surface Bi-O layer is most likely nonmetallic.

We thank R. Collins, S. J. La Placa, R. F. Boehme, T. W. Shaw, and M. W. Shafer for useful discussions. We also thank T. Takahashi and F. J. Himpsel for allowing us to use their PES and IPES spectra for comparison with our STM results.

¹Because of the large number of reported works only one representative reference is given here, Y. Matsui, H. Maeda, Y. Tanaka, and S. Horiuchi, *Jpn. J. Appl. Phys.* **27**, L361 (1988).
²Y. Gao, P. Lee, P. Coppens, M. A. Subramanian, and A. W. Sleight, *Science* **241**, 954 (1988).
³M. D. Kirk, J. Nogami, A. A. Baski, D. B. Mitzi, A. Kapitulnik, T. H. Geballe, and C. F. Quate, *Science* **242**, 1673 (1988).
⁴T. Takahashi, H. Matsuyama, H. Katayama-Yoshida, Y. Okabe, S. Hosoya, K. Seki, H. Fujimoto, M. Sato, and H. Inokuchi, *Nature (London)* **334**, 691 (1988).
⁵W. Drube, F. J. Himpsel, G. V. Chandrashekar, and M. W.

Shafer, *Phys. Rev. B* **39**, 7328 (1989).

⁶J. A. Stroscio, R. M. Feenstra, and A. P. Fein, *Phys. Rev. Lett.* **58**, 1668 (1987); *J. Vac. Sci. Technol. B* **5**, 923 (1987).

⁷P. A. P. Lindberg, Z. X. Shen, B. O. Wells, D. Dessau, D. B. Mitzi, I. Lindau, W. E. Spicer, and A. Kapitulnik, *Phys. Rev. B* **39**, 2890 (1989).

⁸P. Mårtensson and R. M. Feenstra, *Phys. Rev. B* **39**, 7744 (1989). Normalization is performed with 1.5-V broadening of *I/V*.

⁹After this work was completed we learned that Takahashi *et al.* have also obtained a very similar result to ours [T. Takahashi (private communication)].

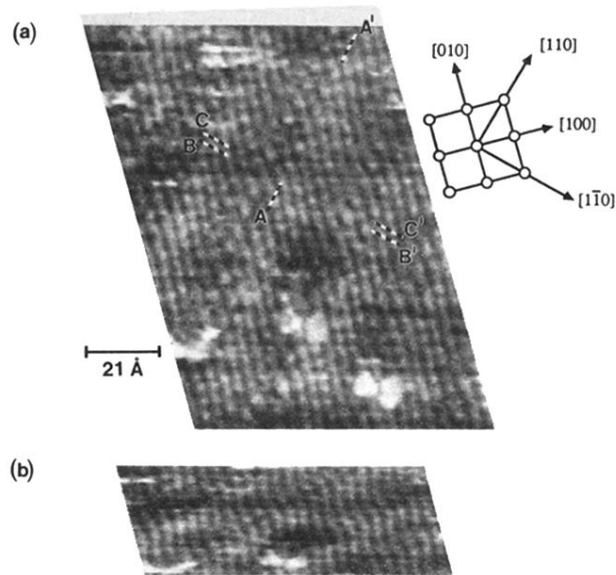


FIG. 1. (a) Top view STM image of a cleaved $\text{Bi}_{2.15}\text{Sr}_{1.7}\text{CaCu}_2\text{O}_{8+\delta}$ surface taken at a sample bias of 1.75 V. The perovskite axes are marked as $[100]$ and $[010]$, and the fundamental tetragonal axes \mathbf{a} and \mathbf{b} are labeled as $[1\bar{1}0]$ and $[110]$, respectively. The surface height is shown with a grey scale, ranging from 0 (black) to 2.5 Å (white). Cross cut AA' is along \mathbf{b} and cross cuts BB' and CC' are along the incommensurate direction \mathbf{a} . (b) The same STM image compressed along the $[010]$ direction.